

# Astrocyte and Neuronal Pannexin I Contribute Distinctly to Seizures

ASN Neuro  
Volume 11: 1–12  
© The Author(s) 2019  
Article reuse guidelines:  
sagepub.com/journals-permissions  
DOI: 10.1177/1759091419833502  
journals.sagepub.com/home/asn



Eliana Scemes<sup>1</sup> , Libor Velíšek<sup>1,2</sup>, and Jana Velíšková<sup>1,3</sup>

## Abstract

ATP- and adenosine-mediated signaling are prominent types of glia–glia and glia–neuron interaction, with an imbalance of ATP/adenosine ratio leading to altered states of excitability, as seen in epileptic seizures. Pannexin I (PanxI), a member of the gap junction family, is an ATP release channel that is expressed in astrocytes and neurons. Previous studies provided evidence supporting a role for purinergic-mediated signaling via PanxI channels in seizures; using mice with global deletion of PanxI, it was shown that these channels contribute in maintenance of seizures by releasing ATP. However, nothing is known about the extent to which astrocyte and neuronal PanxI might differently contribute to seizures. We here show that targeted deletion of PanxI in astrocytes or neurons has opposing effects on acute seizures induced by kainic acid. The absence of PanxI in astrocytes potentiates while the absence of PanxI in neurons attenuates seizure manifestation. Immunohistochemical analysis performed in brains of these mice, revealed that adenosine kinase (ADK), an enzyme that regulates extracellular levels of adenosine, was increased only in seized GFAP-Cre:PanxI<sup>fl/fl</sup> mice. Pretreating mice with the ADK inhibitor, idotubercidin, improved seizure outcome and prevented the increase in ADK immunoreactivity. Together, these data suggest that the worsening of seizures seen in mice lacking astrocyte PanxI is likely related to low levels of extracellular adenosine due to the increased ADK levels in astrocytes. Our study not only reveals an unexpected link between PanxI channels and ADK but also highlights the important role played by astrocyte PanxI channels in controlling neuronal activity.

## Keywords

astrocytes, epilepsy, ion channels, neuro degeneration, neuro glia, neuro signaling

Received December 11, 2018; Received revised January 17, 2019; Accepted for publication February 3, 2019

## Introduction

Purinergic signaling and adenosinergic signaling are emerging as the most prominent types of glia–glia and glia–neuron interaction (Fields and Burnstock, 2006). ATP modulates synaptic strength and plasticity by acting on postsynaptic P2X receptors (Boison et al., 2010), while the action of adenosine relies on adenosine receptors located at presynaptic terminals where they modulate the release of glutamate, gamma-amino-butyric acid (GABA), acetylcholine, and noradrenaline (Boue-Grabot and Pankratov, 2017). Both neurons and astrocytes release ATP by two mechanisms: regulated exocytosis (Coco et al., 2003; Striedinger et al., 2007; Lalo et al., 2014) and diffusion through ion channels (Suadicani et al., 2006; Scemes et al., 2007; Iglesias et al., 2009). In contrast, the source of extracellular adenosine derives from the enzymatic degradation of ATP released by

neurons and astrocytes and from the release of adenosine itself from cells via the equilibrative nucleoside transporters (ENTs; Parkinson et al., 2011). In terms of neuronal excitability, ATP and adenosine have in general opposite effects and an imbalance of ATP/adenosine ratio leads to altered states of excitability. Indeed, impairments in purinergic and adenosinergic signaling have been implicated

<sup>1</sup>Department of Cell Biology and Anatomy, New York Medical College, Valhalla, NY, USA

<sup>2</sup>Departments of Neurology and Pediatrics, New York Medical College, Valhalla, NY, USA

<sup>3</sup>Departments of Obstetrics & Gynecology and Neurology, New York Medical College, Valhalla, NY, USA

### Corresponding Author:

Eliana Scemes, Department of Cell Biology and Anatomy, New York Medical College, Valhalla, NY 10595, USA.

Email: escemes@nycmc.edu



in several neurological conditions including epilepsy (Cunha, 2001; Henshall and Engel, 2015; Boison, 2016; Burnstock, 2017). Because astrocytes are the main cells in the brain to express the enzyme that phosphorylates adenosine into adenosine-mono-phosphate (AMP), adenosine kinase (ADK; Gouder et al., 2004; Fedele et al., 2005; Studer et al., 2006), these cells control brain adenosine tone and thus play an important role in brain physiopathology (Boison, 2013).

Besides the vesicular release of ATP from astrocytes, we found that a plasma membrane channel, Pannexin1 (Panx1), is a site for ATP release from these cells that participates in the intercellular transmission of calcium signals between the cells and is also a key element in inflammasome formation (Suadicani et al., 2006; Scemes et al., 2007; Iglesias et al., 2009). These channels play a role in neuroinflammation, ischemia stroke, seizures, and neuropathic and inflammatory pain (reviewed in Scemes and Veliskova, 2017).

Pannexins (Panxs) are a group of three proteins that share no sequence homology with the chordate gap junction proteins, connexins, but share a low (20%) and significant degree of homology with the invertebrate gap junction proteins, the innexins (Silverman et al., 2009; reviewed in Panchin et al., 2000; Baranova et al., 2004; Panchin, 2005). Panx1 is ubiquitously expressed, forming plasma membrane channels that can be activated by voltage, mechanical stretch, elevated extracellular  $K^+$ , and by intracellular signaling cascade resultant from receptor activation (reviewed in Dahl, 2015). In the central nervous system, Panx1 transcripts and protein are found in astrocytes and in neurons *in vitro* and *in vivo* (Huang et al., 2007; Scemes et al., 2007; Iglesias et al., 2009; Santiago et al., 2011; Hanstein et al., 2013); expression levels are high in the embryonic and young postnatal brain and decline in adulthood (Ray et al., 2005; Vogt et al., 2005).

In hippocampal neurons, Panx1 contributes to N-methyl-D-aspartic acid (NMDA)-mediated epileptiform activity by increasing spike amplitude and decreasing burst intervals (Thompson et al., 2008). In concordance with the proposed role of Panx1 channels in hyperexcitability, our study (Santiago et al., 2011), using mutant mice with global Panx1 deletion, showed that ATP release through these channels contributes to prolonged the clinical manifestations of seizures, status epilepticus (SE). In our acute seizure model performed on juvenile mice, we recorded prolonged SE duration that was paralleled by higher levels of extracellular ATP from brain of wild-type (WT) mice compared with Panx1-null mice and to WT mice treated with Panx1 channel blocker, mefloquine (Santiago et al., 2011). These data led us to hypothesize that Panx1 by releasing ATP contributes to sustain seizures likely due to ATP action on ionotropic P2X receptors. Support for this hypothesis was recently provided in a study performed using resected human epileptic tissues

and in an animal model of temporal lobe epilepsy (Dossi et al., 2018). In this recent study, it was found using electroencephalographic (EEG) recordings in adult mice subjected to intrahippocampal kainic acid (KA) injections that the frequency of spontaneous seizures was greatly reduced in mice with global deletion of Panx1 compared with WT mice and that Panx1 channel blockers (probenecid and mefloquine) reduced the frequency of spontaneous seizures after intraperitoneally (i.p.) injection in WT mice with seizures (Dossi et al., 2018). In addition, in human epileptic tissues, the pro-convulsant effect of ATP released from Panx1 channels was shown to be blunted by inhibiting Panx1 (Dossi et al., 2018).

Thus, these studies provide strong evidence supporting a role for purinergic-mediated signaling via Panx1 channels in seizures. However, nothing is known about the relative contribution of astrocyte versus neuronal Panx1 with regard to seizures. To this end, using transgenic mice with astrocyte (glia fibrillary acid protein: GFAP-Cre) and neuronal (neuro filament H: NFH-Cre) targeted deletion of Panx1, we investigated the impact of these channels on acute seizures induced by KA. We found that differently from neuronal Panx1 channels, astrocyte Panx1 channels delay the progression of acute seizures and improve seizure outcome by modulating the levels of ADK.

## Material and Methods

### Ethics Statement

Mice were housed and maintained under specific pathogen-free conditions in the Animal Resource Facilities of New York Medical College, and all experiments were preapproved by the Institutional Animal Care and Use Committee (IACUC; approval numbers 50-2-0816 and 70-2-1017).

We used mice with cell-type specific deletion of Panx1 generated as previously described (Hanstein et al., 2013, 2016). Briefly, Panx1<sup>fl/fl</sup> mice were generated in our facility from crosses between Panx1<sup>tm1a(KOMP)Wtsi</sup> (obtained from KOMP; RRID:IMSR\_KOMP:CSD66379-1a-Wtsi) and a flippase deleter mouse (B6.ACTFLPe/J; RRID:MGI:5014383) in the C57BL/6 background. For astrocyte and neuronal deletion of Panx1, mGFAP-Cre (B6.Cg-Tg(Gfap-cre)73.12Mvs/J; RRID:MGI:4829613) in the C57BL/6 background and mNFH-Cre (Tg(Nefh-cre)12Kul/J; RRID:MGI:3043822) mice in a mixed (129/Sv\*129S7/SvEvBrd\*C57BL/6\*FVB) background purchased from Jackson laboratory were crossed with Panx1<sup>fl/fl</sup> to generate mGFAP-Cre:Panx1<sup>fl/fl</sup> and mNFH-Cre:Panx1<sup>fl/fl</sup> mice and maintained in our animal facility. To determine the efficiency of recombination, we used the RCE:loxP reporter mice [Gt(ROSA)26Sortm1.1(CAG-EGFP)Fsh; MMRRC Stock No:32037-JAX]

(Sousa et al., 2009), which were bred with either the mGFAP-Cre or the mNFH-Cre lines listed earlier.

All procedures were according to standard animal welfare protocol as authorized by the local veterinary authorities.

### KA-Induced Seizures

Postnatal Day 21 (P21) mice were injected i.p. with KA (20 mg/Kg; Tocris) and maintained in a controlled environment for observation of seizures. Seizure monitoring was done for up to 90 min after KA injection. A subset of mice was subjected to i.p. injection of a blood–brain barrier impermeant adenosine A1 receptor antagonist, 8(p-sulphophenyl)theophylline (8-SPT; 20 mg/Kg; Santa Cruz Biotechnology Inc.) followed by a blood–brain barrier permeant ADK inhibitor, iodotubercidin (itu; 1.0 mg/Kg; Tocris-Biotechnique) 60 min prior to KA administration. After experimentation, a subset of P21 mice was euthanized by decapitation and brains removed, fixed in paraformaldehyde and cryopreserved for immunohistochemistry.

Two independent observers evaluated KA-induced seizure behavior in mice using a scoring system previously described (Santiago et al., 2011): 0 (*normal*), 1 (*frozen and leaning*), 2 (*scratching*), 3 (*forelimb stiff*), 4 (*unilateral forelimb clonus*), 5 (*bilateral forelimb clonus*), 6 (*fore- and hindlimb clonus*), and 7 (*tonic clonic seizures*). Control mice received saline instead of KA. The KA dose used here was chosen because it was the one that produced sustainable SE and had the lowest mortality during observation period.

### EEG Recordings

Mice (P21) were implanted with EEG electrodes using stereotactic apparatus (Heinrich Kopf, Inc.). Mice were first subjected to deep isoflurane anesthesia (5% of isoflurane in O<sub>2</sub> for induction in an induction chamber and 2% isoflurane in O<sub>2</sub> for maintenance using an inhalation mask). Depth of anesthesia was monitored by toe pinch reflex every 5 min. The skull surface was exposed, and holes were drilled for two screws used as a reference and ground electrodes and placed in the nasal bone and behind the lambda, respectively. Silver ball electrodes connected to a dual-in-line connector were used for the cortical recordings and were placed epidurally. The cortical electrodes were positioned symmetrically bilaterally over the sensorimotor (frontal) cortex and over the visual (occipital) cortex. All electrodes including the connector were covered with dental acrylic. After the surgery, the animals were placed on a heating pad until fully ambulatory and then returned to their home cage for 2 days recovery. Sirenia EEG/video monitoring system was used (Pinnacle Technology) for recordings of electrocorticography

(ECoG) response to KA (20 mg/Kg) injection to confirm ictal origin of the behavioral scoring of seizures.

### Western Blot

Mice were anesthetized with isoflurane, decapitated, and brains removed and placed in cold phosphate buffer saline. Whole brains were sonicated in lysis buffer containing protease inhibitors. Each sample (30 µg) was electrophoresed on 4% to 20% gradient sodium dodecyl sulfate-polyacrylamide minigels (BioRad) and transferred to nitrocellulose membranes. Membranes were blocked with 5% milk and incubated for 70 min with antibodies to ADK (1:5,000; Bethyl Cat# A304-280A, RRID: AB\_2620476) or glyceraldehyde 3-phosphate dehydrogenase (1:50,000; Fitzgerald Cat# 10R-G109a, RRID: AB\_1285808). In some experiments, anti-GFAP antibody (1:500; Sigma Cat# SAB4501162, RRID: AB\_10746077) and anti-beta-tubulin antibody (Abcam Cat# ab185057) were used. Horse-radish-peroxidase (HRP)-conjugated goat antimouse and goat anti-rabbit secondary antibodies were used at 1:5,000 (Santa Cruz Biotechnology Cat# sc-2005, RRID: AB\_631736, and Cat# sc-2004, RRID: AB\_631746). Membranes were exposed to enhanced chemiluminescent substrate (Millipore) and detected with X-ray films. Densitometric analysis of bands was performed with ImageJ.

### Immunohistochemistry

Immunostaining was performed according to our standard protocol (Santiago et al., 2011; Hanstein et al., 2013) on sagittal cryosections of paraformaldehyde fixed brains using rabbit anti-ADK antibody (1:1,000; Bethyl Cat# A304-280A, RRID: AB\_2620476) as primary antibody and goat anti-rabbit Alexa Fluor 594 secondary antibody (1:2,000; Molecular Probes Cat# A-11012, RRID: AB\_141359). Immunostained samples were imaged using an Orca-ER charge-coupled device camera (Hamamatsu) attached to an inverted microscope (Eclipse TE-2000; Nikon), equipped with a 20× dry objective and appropriate excitation/emission filter set and Metafluor software version 7.1 (Molecular Devices). Quantification of ADK levels in brain sections was performed on images by measuring ADK immunofluorescence intensity obtained from regions of interest placed on hippocampal and cortical astroglia cells using Metafluor software. Areas of interest were placed in every ADK positive cell present in each brain section (hippocampus and cortex). At least five brain sections per mouse of each genotype were evaluated. In some experiments, brain sections from *Panx1<sup>f/f</sup>*, *GFAP-Cre:Panx1<sup>f/f</sup>*, and *NFH-Cre:Panx1<sup>f/f</sup>* mice were stained using rabbit polyclonal anti-GFAP (1:500; Sigma Cat# SAB4501162, RRID: AB\_10746077) and goat anti-rabbit

Alexa Fluor 488 secondary antibody (1:2,000; Molecular Probes Cat# A-11070, RRID:AB\_142134) to evaluate for possible astrogliosis.

### ATP Release

The amount of ATP released into the artificial cerebrospinal fluid (ACSF) containing 10 mM  $K^+$  ( $10K^+$ -ACSF) from acute brain slices of  $Panx1^{fl/fl}$  and GFAP-Cre:  $Panx1^{fl/fl}$  mice was measured using the luciferin/luciferase assay (Molecular Probes and Promega) and a Turner luminometer, as previously described (Santiago et al., 2011). Fifty microliter of the 5 ml  $10K^+$ -ACSF bathing, the brain slices were collected every 15 min during 1 hr and stored at  $-20^\circ C$  until use. The concentrations of ATP released from brain slices were obtained from standard curves and normalized to the total amount of protein. For that, slices were sonicated in lysis buffer (150 mM NaCl, 10 mM Tris-base, 1% TritonX-100, protease inhibitor cocktail, and pH 7.4) and total protein measured using the bicinonic acid assay (BCA) reagents (Thermo Scientific).

### Dye Uptake

To evaluate the extent of  $Panx1$  activation in acute hippocampal slices of  $Panx1^{fl/fl}$  and NFH-Cre:  $Panx1^{fl/fl}$  mice, we used the dye uptake method (Santiago et al., 2011). Briefly, brain slices of saline and KA-injected mice were incubated for 1 hr, at  $30^\circ C$ , in HEPES-buffered air-bubbled ACSF containing the dye ( $5 \mu M$ ). After three washes with 5 ml ACSF, brain slices were fixed in 4% p-formaldehyde, overnight, at  $4^\circ C$  and then transferred to ice-cold ACSF containing 30% sucrose for few hours. Hippocampal slices were isolated from the surrounding

brain tissue and YoPro1 fluorescence measured from regions of interest placed on the pyramidal cell layer (CA1–CA3) and stratum radiatum of p-formaldehyde fixed tissues using a Nikon inverted microscope equipped with  $4\times$  objective, 488/512 nm filter sets and Metafluor software.

### Statistical Analyses

All statistical analyses were conducted using GraphPad Prism 7.03 software. The area under the curve subroutine of GraphPad Prism was used as an integrated measurement of the overall seizure score. For that, the area was computed using the trapezoid rule which simply connects a straight line between every set of adjacent points defining the curve and sums up the areas beneath these areas. To evaluate the mean differences between treatments and groups, one-way or two-way analysis of variance (ANOVA) followed by Sidak's multiple comparison test was used. In some cases,  $t$  test was employed to compare means between two groups. Data are expressed as mean  $\pm$  standard error of the mean (SEM). Significance level was set at  $p < .05$ .

## Results

### Behavioral and EEG Characterization of KA-Induced Seizures

As expected from our previous work showing that global deletion of  $Panx1$  improved seizure outcome (Santiago et al., 2011), we found that in mice with  $Panx1$  deleted from neurons (NFH-Cre:  $Panx1^{fl/fl}$ ), seizure outcome was significantly better than those recorded from  $Panx1^{fl/fl}$

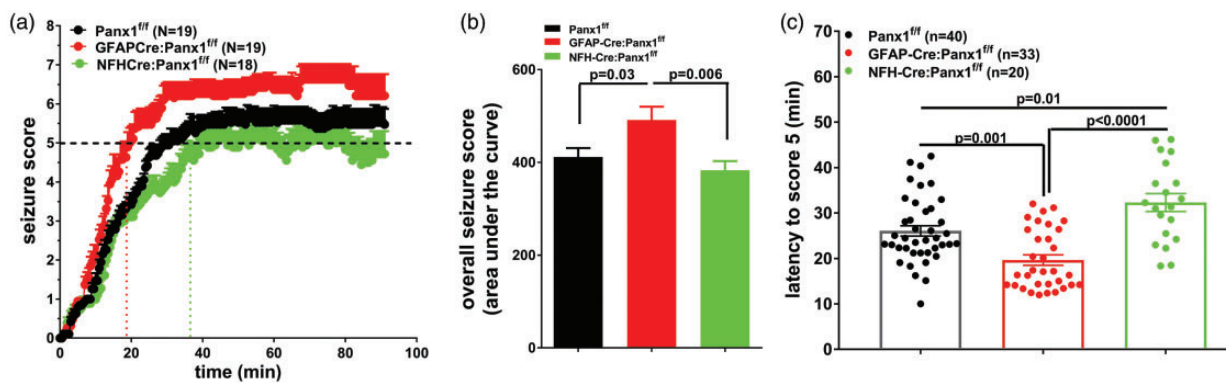


**Figure 1.** Behavioral characterization of KA-induced seizures in mice with cell-type targeted deletion of  $Panx1$ . (a) Time courses of the mean  $\pm$  SEM values of seizure scores measured after intraperitoneal injection of KA in  $Panx1^{fl/fl}$  (black symbols), GFAP-Cre:  $Panx1^{fl/fl}$  (red symbols), and NFH-Cre:  $Panx1^{fl/fl}$  (green symbols) mice. Note that the time to onset of seizure score 5 (bilateral forelimb clonus; dashed black line) of GFAP-Cre:  $Panx1^{fl/fl}$  and that of NFH-Cre:  $Panx1^{fl/fl}$  mice differed (red and green dotted lines). (b) Overall seizure scores (means  $\pm$  SEM) measured by the area under the curves of the time courses of seizure scores displayed in part (a). (c) Mean  $\pm$  SEM values of latencies to reach forelimb clonus (score 5) after intraperitoneal injection of KA in  $Panx1^{fl/fl}$ , GFAP-Cre:  $Panx1^{fl/fl}$ , and NFH-Cre:  $Panx1^{fl/fl}$  mice. The value of  $p$  obtained from one-way ANOVA followed by Sidak's multiple comparison test.  $N$  is the number of mice. GFAP = glia fibrillary acid protein; NFH = neuro filament H.

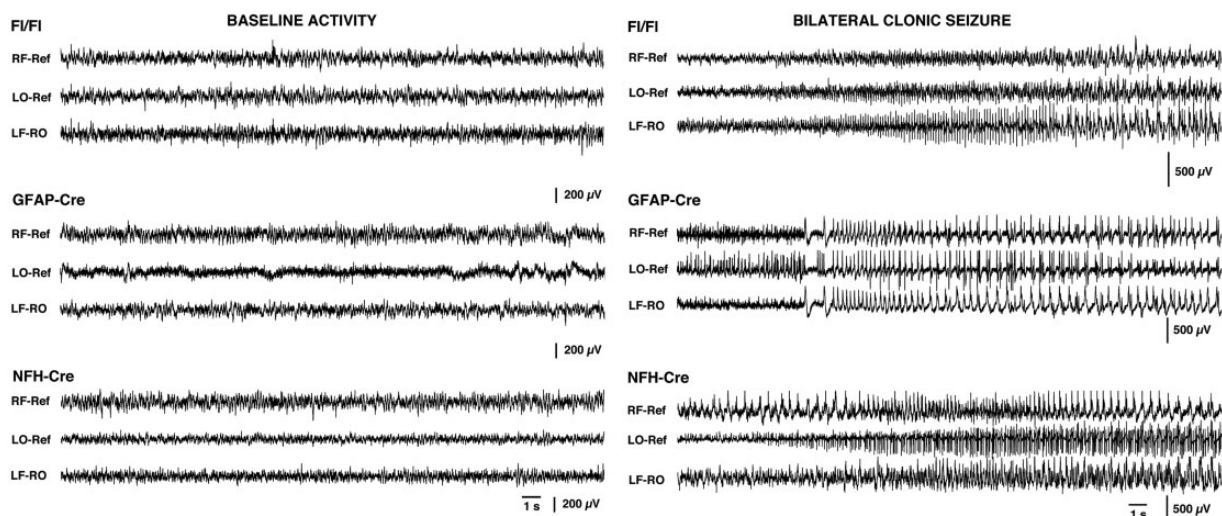
mice. However, we found unexpectedly that mice lacking Panx1 in astrocytes (GFAP-Cre:Panx1<sup>f/f</sup>) had worse seizure scores than control (Panx1<sup>f/f</sup>) KA-injected mice (Figure 1(a)). The overall seizure scores, measured by the area under the curve of the time course of KA-induced seizures, was significantly smaller for NFH-Cre:Panx1<sup>f/f</sup> ( $383.0 \pm 19.7$ ;  $N=17$ ) than that measured from Panx1<sup>f/f</sup> ( $411.5 \pm 19.2$ ;  $N=19$ ), while those measured from GFAP-Cre:Panx1<sup>f/f</sup> ( $491.5 \pm 28.6$ ,  $N=19$ ) were significantly larger than those of Panx1<sup>f/f</sup>, ANOVA:  $F(2, 52)=5.898$ ,  $p=.005$  (Figure 1(b)). In addition to the difference in the overall seizure scores, we found that the latencies to reach bilateral forelimb clonus (seizure score 5) after KA injection were significantly different among the genotypes, ANOVA:  $F(2, 90)=18.8$ ,  $p<.0001$  (Figure 1(c)). While Panx1<sup>f/f</sup> developed bilateral forelimb clonus within  $26.1 \pm 1.2$  min after KA injection, GFAP-Cre:Panx1<sup>f/f</sup> attained this level within  $19.7 \pm 1.1$  min and NFH-Cre:Panx1<sup>f/f</sup> within  $32.3 \pm 2.0$  min (Figure 1(c)). Thus, this data set indicates that compared with Panx1<sup>f/f</sup> mice, the development of bilateral clonic KA-seizures is slower in mice lacking Panx1 in neurons and faster in mice lacking Panx1 in astrocytes.

Figure 2 shows representative EEG recordings obtained from P23 Panx1<sup>f/f</sup>, GFAP-Cre:Panx1<sup>f/f</sup>, NFH-Cre:Panx1<sup>f/f</sup> mice i.p. injected with KA (20 mg/Kg) obtained when mice displayed bilateral forelimb clonus (detected by video monitoring) thus confirming seizures as the electrophysiological correlate of the behavioral scoring. Similarly to the behavioral scoring, EEG

recordings indicated that the latency to onset of SE, defined as continuous ictal events lasting for at least 30 min, was significantly different among the genotypes, ANOVA:  $F(2, 10)=7.4$ ,  $p=.011$ . The onset of SE in NFH-Cre:Panx1<sup>f/f</sup> occurred  $28.4 \pm 4.4$  min ( $N=5$ ) after i.p. injection of KA, which was significantly delayed compared with that recorded from Panx1<sup>f/f</sup> ( $16.8 \pm 0.2$  min,  $N=5$ ; Tukey's multiple comparison test,  $p=.038$ ) and from GFAP-Cre:Panx1<sup>f/f</sup> ( $12.1 \pm 1.4$  min,  $N=3$ ; Tukey's multiple comparison test,  $p=.014$ ).

### Reduced ATP Released From Hippocampal Slices of GFAP-Cre:Panx1<sup>f/f</sup> Mice

We have previously shown that the reduced release of ATP from brain slices of mice with global deletion of Panx1 was associated with an improvement of seizure score in KA-injected mice and hypothesized that the mechanism by which Panx1 channels may contribute to seizures is by increasing the levels of extracellular ATP (Santiago et al., 2011). Thus, according to this hypothesis, it would be expected that mice with cell type targeted deletion of Panx1 would display an improvement of seizure score. Given the result showing that GFAP-Cre:Panx1<sup>f/f</sup> had worst seizures outcomes than predicted, we therefore evaluated for efficient GFAP-Cre-mediated recombination using the RCE:loxP reporter mice (Sousa et al., 2009) and tested whether the amount of ATP released from hippocampal slices of GFAP-Cre:Panx1<sup>f/f</sup> mice was reduced compared with control Panx1<sup>f/f</sup> mice. Image analyses of brain sections



**Figure 2.** Examples of electroencephalographic (EEG) recordings obtained from Panx1<sup>f/f</sup> (F/FI), GFAP-Cre:Panx1<sup>f/f</sup> (GFAP-Cre), and NFH-Cre:Panx1<sup>f/f</sup> (NFH-Cre) mice. The left panel shows baseline EEG activity obtained before kainic acid (KA) i.p. injection, and the right panel depicts ictal activity during bilateral clonic seizure that occurred after KA injection. Bilateral clonic seizures were determined off-line from synchronized video-EEG recordings. LF-Ref = left frontal area (LF) versus reference electrode (Ref); RO-Ref = right occipital area (RO) versus reference electrode (Ref); RF-LO = right frontal area (RF) versus left occipital area (LO; bipolar recording). Calibration bars: 200 μV and 500 μV; time stamp 1 s. GFAP = glia fibrillary acid protein; NFH = neuro filament H.

of mice derived from breeding of mGFAP-Cre X RCE:loxP stained with anti-GFAP antibodies, indicated that 80% to 90% of cells co-expressed enhanced green fluorescent protein (eGFP) and GFAP (data not shown; see also Hanstein et al., 2013, 2016). The extent of recombination is illustrated in Supplemental Figure 1C, and Figure 3(a) shows an image in which few GFAP positive cells were found not to be recombined. Using the luciferin–luciferase assay to measure ATP levels from ACFS bathing  $Panx1^{f/f}$  and GFAP-Cre: $Panx1^{f/f}$  slices exposed to high  $[K^+]$ , we found a significantly lower release of ATP from slices derived from GFAP-Cre: $Panx1^{f/f}$  compared with that of  $Panx1^{f/f}$  mice (Figure 3(b)). These data thus confirmed proper targeted deletion of  $Panx1$  from astrocytes and that  $Panx1$  channels in astrocytes contributed to increase extracellular levels of ATP.

The efficiency of NFH-Cre-mediated recombination in the central nervous system was also evaluated using the RCE:loxP reporter mice (Supplemental Figures 1A, B; see also Hanstein et al., 2013, 2016), and the extent of deletion of  $Panx1$  in mNFH-Cre: $Panx1^{f/f}$  mice was evaluated by the dye uptake approach (see Santiago et al., 2011) using hippocampal slices of saline- and KA-treated mice (Supplemental Figure 1D).

### Increased ADK Immunoreactivity in Brains of GFAP-Cre: $Panx1^{f/f}$ Mice

ADK, a cytosolic enzyme mainly expressed in astrocytes that phosphorylates adenosine to AMP, regulates brain extracellular levels of adenosine, which by acting on A1 adenosine receptors promotes neuronal silencing (Trussell and Jackson, 1985; MacDonald et al., 1986; Dunwiddie and Masino, 2001). To evaluate whether or not the three genotypes displayed distinct ADK expression levels that could explain the difference in seizure outcome observed between GFAP-Cre: $Panx1^{f/f}$  and NFH-Cre: $Panx1^{f/f}$ , western blots and immunohistochemistry were performed in brains of  $Panx1^{f/f}$ , GFAP-Cre: $Panx1^{f/f}$ , and NFH-Cre: $Panx1^{f/f}$  mice treated with saline or KA.

Analysis of Western blots performed on brains of mice treated with KA indicated a significant increase in ADK expression levels in GFAP-Cre: $Panx1^{f/f}$  compared with  $Panx1^{f/f}$  and to NFH-Cre: $Panx1^{f/f}$  mice (Figure 4(a) and (b)); however, no significant difference in ADK expression levels was obtained when saline- and KA-injected mice of the same genotype were compared. Because changes in ADK expression levels induced by KA-seizures were not homogeneous throughout the brain, but more prominent in the affected brain areas, we performed immunohistochemistry on brain sections containing the hippocampus. Indeed, we found that ADK expression levels were not uniform across the brain but were predominantly overexpressed in cortical and hippocampal areas (data not shown) of KA-treated GFAP-Cre: $Panx1^{f/f}$  mice. Thus,

quantification of ADK immunoreactivity was performed only on cortical and hippocampal areas of brain sections of the three mouse genotypes.

Analysis of ADK fluorescence levels obtained from regions of interest (ROIs) placed in all ADK positive cells present in brain sections of three mouse genotypes that were untreated or treated with KA revealed a significant difference in ADK immunoreactivity levels, two-way ANOVA:  $F(2, 22) = 7.535$ ,  $p = 0.0032$  (Figure 4(d)); among the three genotypes, higher ADK immunoreactivity was observed in astrocytes from brains of GFAP-Cre: $Panx1^{f/f}$  (Figure 4(c)). Comparison between saline- and KA-injected mice revealed a significant difference between saline- and KA-treated GFAP-Cre: $Panx1^{f/f}$  mice ( $1.30 \pm 0.05$  fold,  $N = 4$ , Sidak's multiple comparison test:  $p = .0010$ ) but not between saline and KA-treated  $Panx1^{f/f}$  ( $1.13 \pm 0.03$  fold,  $N = 5-8$ , Sidak's multiple comparison test:  $p = .191$ ) and between saline- and KA-treated NFH-Cre: $Panx1^{f/f}$  ( $0.98 \pm 0.02$  fold,  $N = 3-4$ , Sidak's multiple comparison test:  $p > .999$ ; Figure 4(d)). There was no significant difference in ADK immunoreactivity among the three genotypes of saline-injected mice (Figure 4(d);  $p > .999$ ), ruling out a mechanism that could compensate for the loss of  $Panx1$  in these transgenic mouse lines.

This set of data shows that KA-induced seizures leads to changes in ADK immunoreactivity only in GFAP-Cre: $Panx1^{f/f}$  mice, which showed 30% increase in ADK staining following 40 to 50 min SE. These differences in ADK expression thus suggest that in GFAP-Cre: $Panx1^{f/f}$  mice, the levels of extracellular adenosine might be lower than in the two other groups, which could thus account for the faster onset of forelimb clonus and worsen seizure scores in mice lacking  $Panx1$  in astrocytes.

### ADK Inhibition Improves Seizure Outcome in GFAP-Cre: $Panx1^{f/f}$

To evaluate whether or not the degree of ADK immunoreactivity was correlated with seizure outcome or the onset of forelimb clonus, we measured the overall seizure scores and time necessary for mice to attain seizure score of 5 after blocking ADK activity by i.p. injection of ito 1 hr prior to KA injection in  $Panx1^{f/f}$  and GFAP-Cre: $Panx1^{f/f}$  mice. In addition, we performed immunohistochemistry to measure ADK reactivity in brains of these mice. Note that in all cases in which ito was used, mice were treated (i.p. injection) with 8-SPT (an inhibitor of peripheral adenosine A1 receptors) to prevent cardiovascular effects of systemic adenosine (Evoniuk et al., 1987; Nassar and Abdel-Rahman, 2006).

As shown in Figure 5(a), blocking ADK activity significantly improved seizure outcome in GFAP-Cre: $Panx1^{f/f}$  mice to levels similar to those recorded from  $Panx1^{f/f}$  and NFH-Cre: $Panx1^{f/f}$ . The overall seizure

score measured by the area under the curve indicated that there was no significant difference between the three groups, ANOVA:  $F(2, 13) = 2.3$ ,  $p = .14$  (Figure 5(b)). Compared with KA-injected GFAP-Cre:Panx1<sup>f/f</sup> mice (Figure 1), those pretreated with itu displayed a significantly improved overall seizure outcome ( $491.5 \pm 28.6$  vs.  $357.8 \pm 20.1$ ;  $t$  test:  $p = .030$ ; cf. Figures 1 and 5). No significant difference in terms of the overall seizure scores was obtained between KA-injected Panx1<sup>f/f</sup> untreated or treated with itu ( $411.5 \pm 19.2$  vs.  $356.2 \pm 5.7$ ;  $t$  test:  $p = .10$ ) and between KA-injected NFH-Cre:Panx1<sup>f/f</sup> untreated or treated with itu ( $383.0 \pm 16.69$  vs.  $323.0 \pm 4.98$ ;  $t$  test:  $p = .53$ ; cf. Figures 1 and 5). Regarding the latency to bilateral forelimb clonus in animals pretreated with itu, no significant difference was obtained between Panx1<sup>f/f</sup>, GFAP-Cre:Panx1<sup>f/f</sup>, and NFH-Cre:Panx1<sup>f/f</sup> mice, ANOVA:  $F(2, 17) = 1.67$ ,  $p = .22$  (Figure 5(c)). Comparison between itu-treated and itu-untreated mice (see Figures 1 and 5), a significant increase in the time to attain score 5 was recorded in GFAP-Cre:Panx1<sup>f/f</sup> mice, which increased from  $19.7 \pm 1.1$  min ( $N = 33$ ) in KA-injected mice to  $36.1 \pm 4.4$  min ( $N = 8$ ) in itu-pretreated KA-injected mice ( $t$  test:  $p < .0001$ ); no significant differences in the onset to score 5 was recorded from itu-untreated and itu-treated, KA-injected NFH-Cre:Panx1<sup>f/f</sup> mice ( $32.3 \pm 2.0$  min,  $N = 20$  vs.  $29.6 \pm 3.2$  min,  $N = 4$ ;  $t$  test:  $p = .55$ ) and between itu-untreated and itu-treated, KA-injected Panx1<sup>f/f</sup> mice ( $26.8 \pm 1.2$  min,  $N = 40$  vs.  $27.9 \pm 2.6$  min,  $N = 10$ ;  $t$  test:  $p = .41$ ).

Statistical analyses of ADK fluorescence levels obtained from immunohistochemistry of brain sections of KA-injected Panx1<sup>f/f</sup>, GFAP-Cre:Panx1<sup>f/f</sup> and NFH-Cre:Panx1<sup>f/f</sup> mice that were pretreated or untreated with itu revealed a significant difference among the groups

(two-way ANOVA:  $F(2, 21) = 6.139$ ,  $p = .0080$ ) (Figure 5(d)). Compared with KA-injected mice, itu pretreatment reduced ADK immunoreactivity in GFAP-Cre:Panx1<sup>f/f</sup> mice from  $1.26 \pm 0.05$  ( $N = 4$ ) to  $1.01 \pm 0.03$  ( $N = 6$ ; Sidak's multiple comparison test:  $p = .0002$ ) and did not alter ADK immunoreactivity in Panx1<sup>f/f</sup> ( $1.13 \pm 0.06$  fold,  $N = 5$  vs.  $1.12 \pm 0.01$  fold,  $N = 5$ ,  $p = .99$ ) or NFH-Cre:Panx1<sup>f/f</sup> mice ( $0.97 \pm 0.02$  fold,  $N = 4$  to  $0.94 \pm 0.01$  fold,  $N = 3$ ,  $p = .90$ ; Figure 5(d)).

Together, the data indicate that seizure outcome and time to onset of bilateral forelimb clonus are correlated with the degree of ADK expression and that astrocyte Panx1 plays an important role in this relationship. A putative model for the underlying mechanism involved in this process is shown in Figure 6 (see "Discussion" section).

## Discussion

Imbalance of excitatory and inhibitory neurotransmission is considered a hallmark of seizure generation and epilepsy development. Besides the glutamate and GABA neuro-axis, dysregulation of purinergic (ATP) and adenosinergic (adenosine) signaling has been implicated in epileptic seizures (Wieraszko et al., 1989; Wieraszko and Seyfried, 1989; Dale and Freguelli, 2009). Neurons and astrocytes can release ATP via regulated secretion (Coco et al., 2003; Pankratov et al., 2006; Bowser and Khakh, 2007; Boue-Grabot and Pankratov, 2017) and via diffusion through ion channels, such as Panx1 (Bao et al., 2004; Scemes et al., 2007; Iglesias et al., 2009). The source of extracellular adenosine, however, relies on the breakdown of ATP by ectonucleotidases and the transport of adenosine via ENTs, with the direction of adenosine flux dictated by ADK activity.

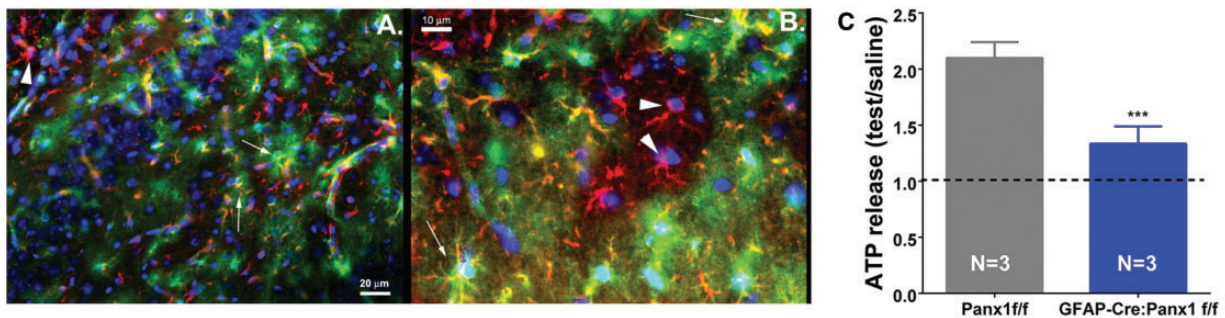


**Figure 3.** Reduced ATP release from hippocampal slices of mice lacking Panx1 from astrocytes. (a and b) Epifluorescence images, (a) 20 $\times$  and (b) 40 $\times$ , of 4% p-formaldehyde fixed hippocampal slices derived from P14 mGFAP-Cre:RCE mice showing the efficacy of Cre recombination in GFAP positive cells of stratum radiatum. Arrows indicate cells that were recombined and thus coexpress eGFP (green) and GFAP (red), and arrowheads indicate cells that were not recombined and thus express only GFAP. The RCE:loxP reporter mice (Sousa et al., 2009) were bred with the mGFAP-Cre line used to target the deletion of Panx1 in astrocytes using Panx1<sup>f/f</sup> mice. Images were acquired using an inverted epifluorescence Eclipse Nikon microscope equipped with 20 $\times$  and 40 $\times$  objectives controlled by Metafluor software. (c) Histograms of the relative mean  $\pm$  SEM values of ATP in the medium released from Panx1<sup>f/f</sup> (gray bar) and mGFAP-Cre:Panx1<sup>f/f</sup> (blue bar) brain slices that were exposed for 1 hr to 10 mM K<sup>+</sup> ACSF. N is the number of animals used. \*\*\* $p < .001$  ( $t$  test). GFAP = glia fibrillary acid protein.

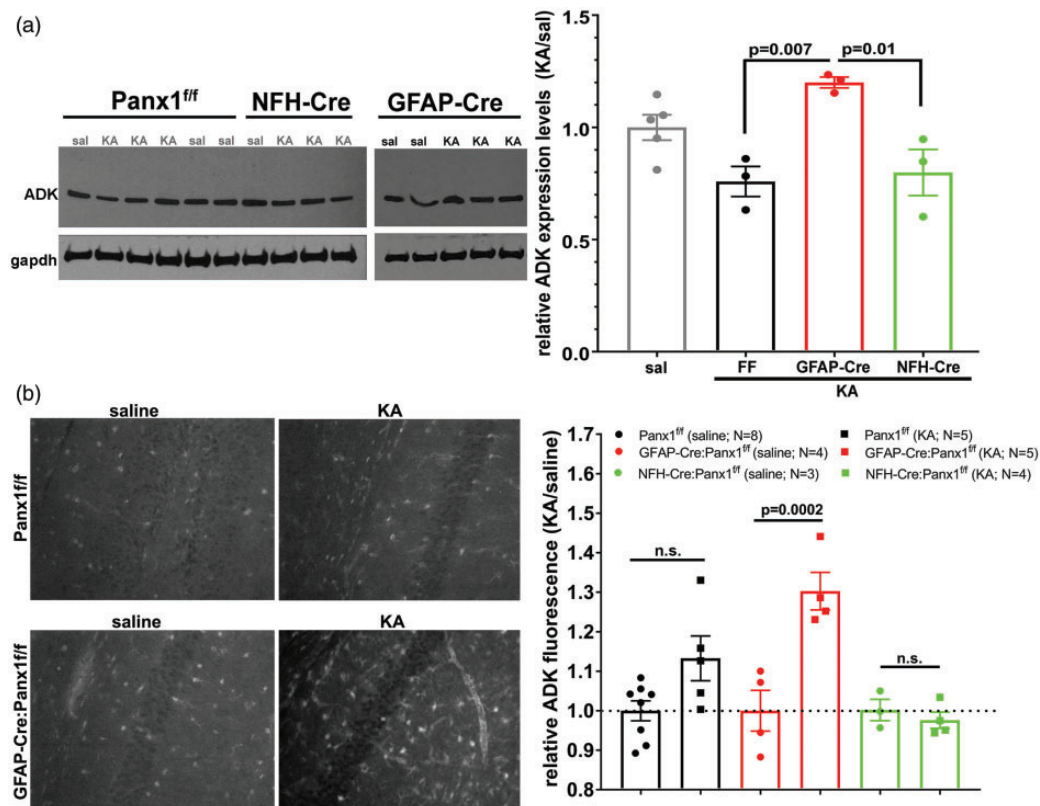


**Figure 4.** ADK expression levels. (a, left) Western blots showing the expression levels of ADK in whole brain homogenates of saline (sal) and KA injected *Panx1<sup>ff</sup>*, *NFH-Cre:Panx1<sup>ff</sup>*, and *GFAP-Cre:Panx1<sup>ff</sup>* mice. Glyceraldehyde 3-phosphate dehydrogenase (GAPDH) was used as an internal control. (a, right) Relative mean  $\pm$  SEM values of ADK expression levels obtained from densitometric analysis of western blots of brain homogenates displayed in the left panel. The values of  $p$  were obtained from one-way ANOVA followed by Tukey's multiple comparison test. (b, left) Representative images of brain sections immunostained using anti-ADK antibodies obtained from saline- and KA-injected *Panx1<sup>ff</sup>* and *GFAP-Cre:Panx1<sup>ff</sup>* mice. Note that high levels of immunoreactivity following KA treatment in *GFAP-Cre:Panx1<sup>ff</sup>* compared with *Panx1<sup>ff</sup>* mice. (b, right) Relative mean  $\pm$  SEM values of ADK fluorescence obtained from images of brain sections of *Panx1<sup>ff</sup>*, *GFAP-Cre:Panx1<sup>ff</sup>*, and *NFH-Cre:Panx1<sup>ff</sup>* mice 40 to 60 min after KA-induced bilateral forelimb clonus (square) compared with saline injected mice (circles). The values of  $p$  were obtained from two-way ANOVA followed by Sidak's multiple comparison test.  $N$  = number of mice; GFAP = glia fibrillary acid protein; NFH = neuro filament H; KA = kainic acid; ADK = adenosine kinase.

It has been hypothesized that depending on the spatial and temporal distribution of released ATP, the resulting effect on synaptic activity could be excitatory or inhibitory (Kumaria et al., 2008); indeed, it has been shown that the immediate and localized action of ATP is excitatory such as that occurring at postsynaptic P2X receptors that promotes alpha-amino-3-hydroxy-5-methyl-4-isoxazolepropionic acid (AMPA) receptor insertion or downregulation of GABA-A receptors (Pankratov et al., 1998; Gordon et al., 2005, review in Boue-Grabot and Pankratov, 2017), while for actions at longer distance, ATP would be inhibitory because it is degraded to adenosine, as reported for glia ATP inhibiting neuronal activity (Newman, 2003; Wall and Dale, 2013).

Despite the inhibitory action of ATP, there is strong evidence that the overall effect of this purine is excitatory at least with regard to epileptic seizures. Evidence that ATP is involved in hyperexcitability comes from

experiments showing generation and augmentation of seizures after ATP microinjections into specific brain areas (Engel et al., 2012, 2016), from studies showing increased extracellular levels of ATP in the brains of seizure prone mice and of mice i.p. injected with KA (Wieraszko and Seyfried, 1989; Santiago et al., 2011). In addition, it was shown that in patients with epilepsy, ATP levels released from resected brain tissues increased 1.5-fold following ictal discharges (Dossi et al., 2018).

Among the pathways involved in the release of ATP, there is evidence for the involvement of Panx1 channels. Several studies have indicated that the ATP release channels Panx1 play a role in epileptic seizures, which has been reported to provide either excitatory or inhibitory drive (Zappala et al., 2006; Thompson et al., 2008; Kawamura et al., 2010; Mylvaganam et al., 2010; Kim and Kang, 2011; Santiago et al., 2011; Lopatar et al., 2015; Li et al., 2017; Scemes and Veliskova, 2017;

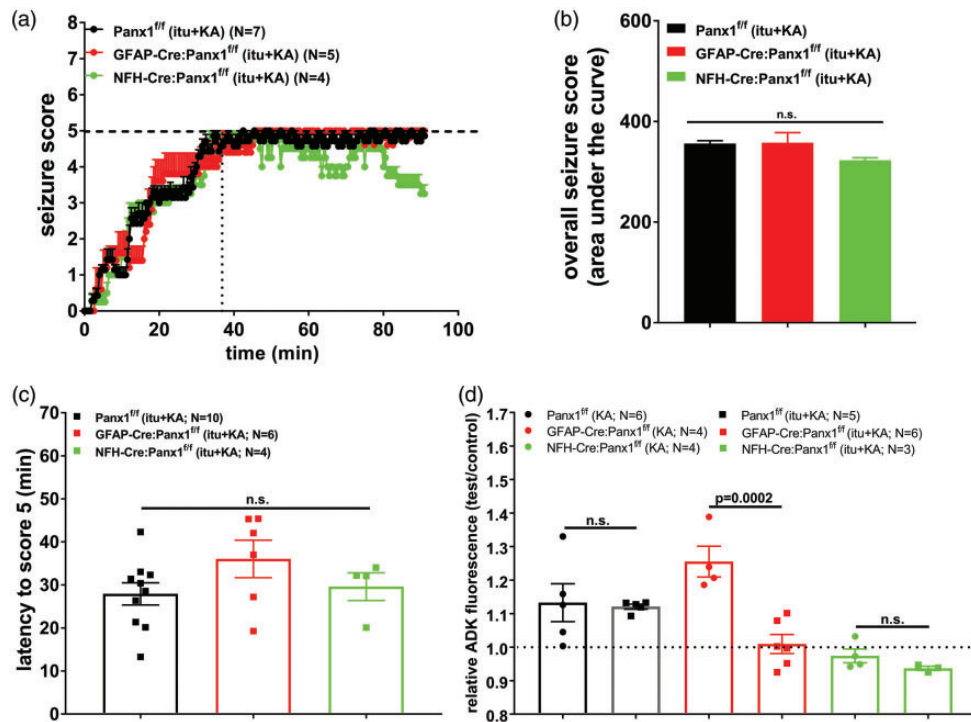


**Figure 5.** Inhibition of ADK improves seizure outcome and prevents the increase in ADK in GFAP-Cre:Panx1<sup>fl/fl</sup> mice. (a) Time courses of the mean  $\pm$  SEM values of seizure scores measured after intraperitoneal injection of KA in Panx1<sup>fl/fl</sup> (black symbols), GFAP-Cre:Panx1<sup>fl/fl</sup> (red symbols), and NFH-Cre:Panx1<sup>fl/fl</sup> mice (green symbols) pretreated with idotubercidin (itu) in the presence of 8-SPT. Note that the time to onset to score 5 (black dotted line) was similar among the three mouse genotypes. (b) Overall seizure scores measured by the area under the curves of the time courses of seizure scores displayed in part (a); note that the overall seizure score of GFAP-Cre:Panx1<sup>fl/fl</sup> mice was not significantly different from the other genotypes. (c) Mean  $\pm$  SEM latency values for mice to reach forelimb clonus (score 5) after intraperitoneal injection of KA in Panx1<sup>fl/fl</sup>, GFAP-Cre:Panx1<sup>fl/fl</sup>, and NFH-Cre:Panx1<sup>fl/fl</sup> pretreated with itu. (d) Relative (test/saline) mean  $\pm$  SEM values of ADK fluorescence levels obtained from brain section of KA-injected and itu-untreated (circles) and KA-injected and itu-treated mice (squares). The values of *p* obtained from one-way (b and c) and two-ways ANOVA (d) followed by Sidak's multiple comparison test. *N* = number of mice; GFAP = glia fibrillary acid protein; NFH = neuro filament H; KA = kainic acid; ADK = adenosine kinase.

Dossi et al., 2018). For instance, activation of neuronal Panx1 channels has been implicated in the maintenance of N-methyl-D-aspartic acid (NMDA)- and KA-induced seizure activity either by promoting depolarization or by the activation of ionotropic P2X receptors (Thompson et al., 2008; Santiago et al., 2011). On the other hand, under hypoglycemia or in the pilocarpine model, open Panx1 channel has been proposed to prevent seizure by activating neuronal adenosine receptors (AR) or by desensitizing muscarinic receptors (Kawamura et al., 2010; Kim and Kang, 2011).

These distinct functional outcomes may be related to the different models used, to the divergent effects of ATP on synaptic activity, or to the cell type that releases ATP. Using mice with targeted deletion of Panx1 from astrocytes or neurons, we investigated the relative contribution of astrocytes and neuronal Panx1 to acute seizures using the KA model in juvenile mice. We found that the presence of the ATP release Panx1 channels in astrocytes confers protection in terms of the overall seizure outcome and the time course with which bilateral clonic seizures

developed, while the presence of neuronal Panx1 produced opposite outcomes.

These results are unexpected given that we and others have found that Panx1-mediated ATP release prolonged seizure activity and that there is a positive correlation between the levels of ATP released and seizure activity/outcome (Santiago et al., 2011; Dossi et al., 2018). Thus, it would be expected that deleting Panx1 from neurons or from astrocytes would result in lower overall levels of released ATP and improvement of seizure scores, albeit not as intense as that seen in global Panx1 knock-out mice (Santiago et al., 2011; Dossi et al., 2018). The possibility that GFAP-Cre-mediated recombination was inefficient was ruled out as we found 80% to 90% cells co-expressing eGFP and GFAP (see also Figure 3(a), Supplemental Figure 1, (Hanstein et al., 2013, 2016); moreover, we confirmed that GFAP-Cre:Panx1<sup>fl/fl</sup> brain slices released less ATP than control mice (Figure 3(b)). To explain our finding that the GFAP-Cre:Panx1<sup>fl/fl</sup> mice have worse seizure scores than the Panx1<sup>fl/fl</sup> and NFH-Cre:Panx1<sup>fl/fl</sup> mice, despite their lower levels of ATP

released, we hypothesized that levels of the anticonvulsant adenosine might be compromised. Because astrocytes are the main cells in the brain to express ADK, an enzyme that controls extracellular levels of adenosine (Boison, 2012), and because changes in ADK have been linked to seizures (Gouder et al., 2004; Fedele et al., 2005; Aronica et al., 2011), we investigated the expression of this enzyme in brains of these mice. Our results showed increased levels of ADK only in GFAP-Cre:Panx1<sup>f/f</sup> mouse brains and only after sustained SE. Further support to the hypothesis that increased ADK was related to the outcomes was obtained by blocking ADK activity with itu, showing that this blocker prevented the increase in ADK and reverted the effects of KA-treated to that seen in saline-injected GFAP-Cre:Panx1<sup>f/f</sup> mice.

Changes in ADK expression levels following intrahippocampal KA injection has been reported to be biphasic, with an initial decrease in ADK expression followed by a gradual increase that peaks at 4 weeks after injection, a time point that corresponds to the occurrence of spontaneous recurrent seizures and is paralleled by astrogliosis (Gouder et al., 2004). Although we did not observe any significant decrease in ADK expression levels in our experiment, which could be model dependent, we found in agreement with Gouder et al. (2004) that overexpression of ADK in the GFAP-Cre:Panx1<sup>f/f</sup> mice was paralleled by astrogliosis, as seen by intense GFAP immunoreactivity (Supplemental Figure 2). Astrogliosis was not present in neither Panx1<sup>f/f</sup> nor NFH-Cre:Panx1<sup>f/f</sup> mice (Supplemental Figure 2). This suggests that mice lacking astrocyte Panx1 are more likely to be prone to injury induced astrogliosis and to develop spontaneous recurrent seizures. Such possibilities should be further investigated.

The mechanism that we hypothesized to underlie the differential effects of astrocytes and neuronal Panx1 in acute seizure severity is illustrated in Figure 6. In the absence of Panx1 channels in astrocytes (GFAP-Cre:Panx1<sup>f/f</sup>), intracellular levels of ATP are expected to be higher given that this purine is not released through these channels. This enhanced [ATP]<sub>i</sub> in astrocytes favor the phosphorylation of intracellular adenosine to AMP mediated by ADK (Rotllan and Miras Portugal, 1985). As a consequence, intracellular levels of adenosine decrease, favoring the influx of extracellular adenosine via the ENTs (Griffith and Jarvis, 1996; Boswell-Casteel and Hays, 2017), thus reducing the impact of adenosinergic signaling on neuronal excitability. In contrast, the absence of neuronal Panx1, the levels of extracellular adenosine could rise due to enzymatic degradation of ATP released by astrocytes and by the efflux of adenosine through astrocyte ENTs, due to the reduced ADK activity, thus enhancing adenosinergic signaling. This model implies that astrocyte Panx1 channels by modulating ADK activity dictate the direction of the imbalance between ATP/adenosine and excitation/inhibition.

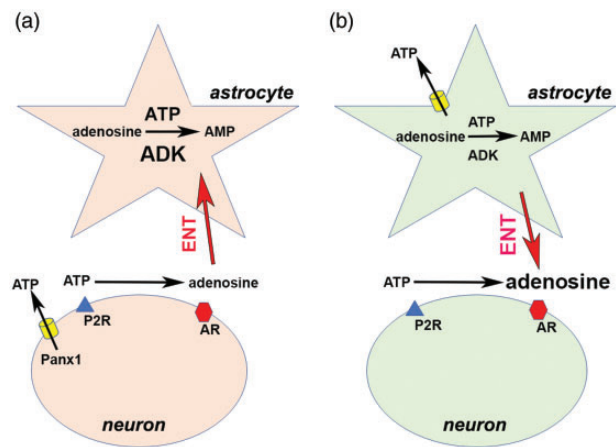


**Figure 6.** Hypothetical mechanism underlying the impact of astrocyte and neuronal Panx1 channels to seizures. (a) In the absence of Panx1 in astrocytes (GFAP-Cre:Panx1<sup>f/f</sup>), the observed increased levels of ADK together with the supposedly higher levels of intracellular ATP in the astrocytic compartment would favor the phosphorylation of adenosine to AMP, reducing intracellular levels of adenosine. Under this condition, the net flux of adenosine through ENTs would be inward, thus reducing the extracellular levels of adenosine. The resultant imbalance of ATP to adenosine ratio would then favor hyperexcitability. (b) In the absence of neuronal Panx1 channels (NFH-Cre:Panx1<sup>f/f</sup>), the reduced levels of intracellular ADK and ATP would reduce adenosine phosphorylation, and the accumulated adenosine could then be transported out of the astrocytic compartment, increasing the extracellular levels of adenosine. Under this condition, the imbalance in ATP to adenosine ratio would favor decreased excitability. ADK = adenosine kinase; GFAP = glia fibrillary acid protein; NFH = neuro filament H; AMP = adenosine-mono-phosphate; AR = adenosine receptors; ENT = equilibrative nucleoside transporter.

## Summary

(a) In contrast to neurons, astrocyte Panx1 delays seizure progression and improves outcome; (b) high levels of adenosine kinase occur in brains lacking Panx1 in astrocytes; and (c) astrocyte Panx1 dictates the direction of the imbalance between ATP/adenosine and excitation/inhibition.

## Acknowledgments

The authors are grateful to Drs Detlev Boison (Legacy Research Institute, OR) and David C. Spray (Albert Einstein College of Medicine, NY) for their comments and suggestions given to the work. The authors acknowledge the contribution of Mr. Jian Pan for his technical support and for maintaining mouse colonies.

## Declaration of Conflicting Interests

The author(s) declared no potential conflicts of interest with respect to the research, authorship, and/or publication of this article.

## Funding

The author(s) disclosed receipt of the following financial support for the research, authorship, and/or publication of this article: This work was supported by the National Institute of Neurological Disorders and Stroke of the National Institutes of Health (5R01NS092786).

## ORCID iD

Eliana Scemes  <http://orcid.org/0000-0002-6650-3976>

## Supplemental Material

Supplemental material for this article is available online.

## References

- Aronica, E., Zurolo, E., Iyer, A., de Groot, M., Anink, J., Carbonell, C., van Vliet, E. A., Baayen, J. C., Boison, D., & Gorter, J. A. (2011). Upregulation of adenosine kinase in astrocytes in experimental and human temporal lobe epilepsy. *Epilepsia*, *52*, 1645–1655.
- Bao, L., Locovei, S., & Dahl, G. (2004). Pannexin membrane channels are mechanosensitive conduits for ATP. *FEBS Lett*, *572*, 65–68.
- Baranova, A., Ivanov, D., Petrash, N., Pestova, A., Skoblov, M., Kelmanson, I., Shagin, D., Nazarenko, S., Geraymovych, E., Litvin, O., Tiunova, A., Born, T. L., Usman, N., Staroverov, D., Lukyanov, S., & Panchin, Y. (2004). The mammalian pannexin family is homologous to the invertebrate innexin gap junction proteins. *Genomics*, *83*, 706–716.
- Boison, D. (2012). Adenosine dysfunction in epilepsy. *Glia*, *60*, 1234–1243.
- Boison, D. (2013). Adenosine kinase: Exploitation for therapeutic gain. *Pharmacol Rev*, *65*, 906–943.
- Boison, D. (2016). Adenosinergic signaling in epilepsy. *Neuropharmacology*, *104*, 131–139.
- Boison, D., Chen, J. F., & Fredholm, B. B. (2010). Adenosine signaling and function in glial cells. *Cell Death Differ*, *17*, 1071–1082.
- Boswell-Casteel, R. C., & Hays, F. A. (2017). Equilibrative nucleoside transporters—A review. *Nucleosides Nucleotides Nucleic Acids*, *36*, 7–30.
- Boue-Grabot, E., & Pankratov, Y. (2017). Modulation of central synapses by astrocyte-released ATP and postsynaptic P2X receptors. *Neural Plast*, *2017*, 9454275.
- Bowser, D. N., & Khakh, B. S. (2007). Vesicular ATP is the predominant cause of intercellular calcium waves in astrocytes. *J Gen Physiol*, *129*, 485–491.
- Burnstock, G. (2017). Purinergic signalling and neurological diseases: An update. *CNS Neurol Disord Drug Targets*, *16*, 257–265.
- Coco, S., Calegari, F., Pravettoni, E., Pozzi, D., Taverna, E., Rosa, P., Matteoli, M., & Verderio, C. (2003). Storage and release of ATP from astrocytes in culture. *J Biol Chem*, *278*, 1354–1362.
- Cunha, R. A. (2001). Adenosine as a neuromodulator and as a homeostatic regulator in the nervous system: Different roles, different sources and different receptors. *Neurochem Int*, *38*, 107–125.
- Dahl, G. (2015). ATP release through pannexon channels. *Philos Trans R Soc Lond B Biol Sci*, *370*, pii: 20140191.
- Dale, N., & Frenguelli, B. G. (2009). Release of adenosine and ATP during ischemia and epilepsy. *Curr Neuropharmacol*, *7*, 160–179.
- Dossi, E., Blauwblomme, T., Moulard, J., Chever, O., Vasile, F., Guinard, E., Le Bert, M., Couillin, I., Pallud, J., Capelle, L., Huberfeld, G., & Rouach, N. (2018). Pannexin-1 channels contribute to seizure generation in human epileptic brain tissue and in a mouse model of epilepsy. *Sci Transl Med*, *10*, pii: eaar3796.
- Dunwiddie, T. V., & Masino, S. A. (2001). The role and regulation of adenosine in the central nervous system. *Annu Rev Neurosci*, *24*, 31–55.
- Engel, T., Alves, M., Sheedy, C., & Henshall, D. C. (2016). ATPergic signalling during seizures and epilepsy. *Neuropharmacology*, *104*, 140–153.
- Engel, T., Gomez-Villafuertes, R., Tanaka, K., Mesuret, G., Sanz-Rodriguez, A., Garcia-Huerta, P., Miras-Portugal, M. T., Henshall, D. C., & Diaz-Hernandez, M. (2012). Seizure suppression and neuroprotection by targeting the purinergic P2X7 receptor during status epilepticus in mice. *FASEB J*, *26*, 1616–1628.
- Evoniuk, G., von Borstel, R. W., & Wurtman, R. J. (1987). Antagonism of the cardiovascular effects of adenosine by caffeine or 8-(p-sulfophenyl)theophylline. *J Pharmacol Exp Ther*, *240*, 428–432.
- Fedele, D. E., Gouder, N., Guttinger, M., Gabernet, L., Scheurer, L., Rulicke, T., Crestani, F., & Boison, D. (2005). Astroglialosis in epilepsy leads to overexpression of adenosine kinase, resulting in seizure aggravation. *Brain*, *128*, 2383–2395.
- Fields, R. D., & Burnstock, G. (2006). Purinergic signalling in neuron-glia interactions. *Nat Rev Neurosci*, *7*, 423–436.
- Gordon, G. R., Baimoukhametova, D. V., Hewitt, S. A., Rajapaksha, W. R., Fisher, T. E., & Bains, J. S. (2005). Norepinephrine triggers release of glial ATP to increase postsynaptic efficacy. *Nat Neurosci*, *8*, 1078–1086.
- Gouder, N., Scheurer, L., Fritschy, J. M., & Boison, D. (2004). Overexpression of adenosine kinase in epileptic hippocampus contributes to epileptogenesis. *J Neurosci*, *24*, 692–701.
- Griffith, D. A., & Jarvis, S. M. (1996). Nucleoside and nucleobase transport systems of mammalian cells. *Biochim Biophys Acta*, *1286*, 153–181.
- Hanstein, R., Hanani, M., Scemes, E., & Spray, D. C. (2016). Glial pannexin1 contributes to tactile hypersensitivity in a mouse model of orofacial pain. *Sci Rep*, *6*, 38266.
- Hanstein, R., Negoro, H., Patel, N. K., Charollais, A., Meda, P., Spray, D. C., Suadicani, S. O., & Scemes, E. (2013). Promises and pitfalls of a Pannexin1 transgenic mouse line. *Front Pharmacol*, *4*, 61.
- Henshall, D. C., & Engel, T. (2015). P2X purinoceptors as a link between hyperexcitability and neuroinflammation in status epilepticus. *Epilepsy Behav*, *49*, 8–12.
- Huang, Y. J., Maruyama, Y., Dvoryanchikov, G., Pereira, E., Chaudhari, N., & Roper, S. D. (2007). The role of pannexin 1

- hemichannels in ATP release and cell-cell communication in mouse taste buds. *Proc Natl Acad Sci U S A*, *104*, 6436–6441.
- Iglesias, R., Dahl, G., Qiu, F., Spray, D. C., & Scemes, E. (2009). Pannexin 1: The molecular substrate of astrocyte “hemichannels.” *J Neurosci*, *29*, 7092–7097.
- Kawamura, M., Jr., Ruskin, D. N., & Masino, S. A. (2010). Metabolic autocrine regulation of neurons involves cooperation among pannexin hemichannels, adenosine receptors, and KATP channels. *J Neurosci*, *30*, 3886–3895.
- Kim, J. E., & Kang, T. C. (2011). The P2X7 receptor-pannexin-1 complex decreases muscarinic acetylcholine receptor-mediated seizure susceptibility in mice. *J Clin Invest*, *121*, 2037–2047.
- Kumaria, A., Tolia, C. M., & Burnstock, G. (2008). ATP signalling in epilepsy. *Purinergic Signal*, *4*, 339–346.
- Lalo, U., Rasooli-Nejad, S., & Pankratov, Y. (2014). Exocytosis of gliotransmitters from cortical astrocytes: Implications for synaptic plasticity and aging. *Biochem Soc Trans*, *42*, 1275–1281.
- Li, S., Zang, Z., He, J., Chen, X., Yu, S., Pei, Y., Hou, Z., An, N., Yang, H., Zhang, C., & Liu, S. (2017). Expression of pannexin 1 and 2 in cortical lesions from intractable epilepsy patients with focal cortical dysplasia. *Oncotarget*, *8*, 6883–6895.
- Lopatar, J., Dale, N., & Frenguelli, B. G. (2015). Pannexin-1-mediated ATP release from area CA3 drives mGlu5-dependent neuronal oscillations. *Neuropharmacology*, *93*, 219–228.
- MacDonald, R. L., Skerritt, J. H., & Werz, M. A. (1986). Adenosine agonists reduce voltage-dependent calcium conductance of mouse sensory neurones in cell culture. *J Physiol*, *370*, 75–90.
- Mylvaganam, S., Zhang, L., Wu, C., Zhang, Z. J., Samoilova, M., Eubanks, J., Carlen, P. L., & Poulter, M. O. (2010). Hippocampal seizures alter the expression of the pannexin and connexin transcriptome. *J Neurochem*, *112*, 92–102.
- Nassar, N., & Abdel-Rahman, A. A. (2006). Central adenosine signaling plays a key role in centrally mediated hypotension in conscious aortic barodenervated rats. *J Pharmacol Exp Ther*, *318*, 255–261.
- Newman, E. A. (2003). Glial cell inhibition of neurons by release of ATP. *J Neurosci*, *23*, 1659–1666.
- Panchin, Y. V. (2005). Evolution of gap junction proteins—the pannexin alternative. *J Exp Biol*, *208*, 1415–1419.
- Panchin, Y. V., Kelmanson, I., Matz, M., Lukyanov, K., Usman, N., & Lukyanov, S. (2000). A ubiquitous family of putative gap junction molecules. *Curr Biol*, *10*, R473–R474.
- Pankratov, Y., Castro, E., Miras-Portugal, M. T., & Krishtal, O. (1998). A purinergic component of the excitatory postsynaptic current mediated by P2X receptors in the CA1 neurons of the rat hippocampus. *Eur J Neurosci*, *10*, 3898–3902.
- Pankratov, Y., Lalo, U., Verkhratsky, A., & North, R. A. (2006). Vesicular release of ATP at central synapses. *Pflugers Arch*, *452*, 589–597.
- Parkinson, F. E., Damaraju, V. L., Graham, K., Yao, S. Y., Baldwin, S. A., Cass, C. E., & Young, J. D. (2011). Molecular biology of nucleoside transporters and their distributions and functions in the brain. *Curr Top Med Chem*, *11*, 948–972.
- Ray, A., Zoidl, G., Weickert, S., Wahle, P., & Dermietzel, R. (2005). Site-specific and developmental expression of pannexin1 in the mouse nervous system. *Eur J Neurosci*, *21*, 3277–3290.
- Rotllan, P., & Miras Portugal, M. T. (1985). Adenosine kinase from bovine adrenal medulla. *Eur J Biochem*, *151*, 365–371.
- Santiago, M. F., Veliskova, J., Patel, N. K., Lutz, S. E., Caille, D., Charollais, A., Meda, P., & Scemes, E. (2011). Targeting pannexin1 improves seizure outcome. *PLoS One*, *6*, e25178.
- Scemes, E., Suadicani, S. O., Dahl, G., & Spray, D. C. (2007). Connexin and pannexin mediated cell-cell communication. *Neuron Glia Biol*, *3*, 199–208.
- Scemes, E., & Veliskova, J. (2017). Exciting and not so exciting roles of pannexins. *Neurosci Lett*, S0304-3940(17)30220-3.
- Silverman, W. R., de Rivero Vaccari, J. P., Locovei, S., Qiu, F., Carlsson, S. K., Scemes, E., Keane, R. W., & Dahl, G. (2009). The pannexin 1 channel activates the inflammasome in neurons and astrocytes. *J Biol Chem*, *284*, 18143–18151.
- Sousa, V. H., Miyoshi, G., Hjerling-Leffler, J., Karayannis, T., & Fishell, G. (2009). Characterization of Nkx6-2-derived neocortical interneuron lineages. *Cereb Cortex*, *19*, i1–i10.
- Striedinger, K., Meda, P., & Scemes, E. (2007). Exocytosis of ATP from astrocyte progenitors modulates spontaneous Ca<sup>2+</sup> oscillations and cell migration. *Glia*, *55*, 652–662.
- Studer, F. E., Fedele, D. E., Marowsky, A., Schwerdel, C., Wernli, K., Vogt, K., Fritschy, J. M., & Boison, D. (2006). Shift of adenosine kinase expression from neurons to astrocytes during postnatal development suggests dual functionality of the enzyme. *Neuroscience*, *142*, 125–137.
- Suadicani, S. O., Brosnan, C. F., & Scemes, E. (2006). P2X7 receptors mediate ATP release and amplification of astrocytic intercellular Ca<sup>2+</sup> signaling. *J Neurosci*, *26*, 1378–1385.
- Thompson, R. J., Jackson, M. F., Olah, M. E., Rungta, R. L., Hines, D. J., Beazely, M. A., MacDonald, J. F., & MacVicar, B. A. (2008). Activation of pannexin-1 hemichannels augments aberrant bursting in the hippocampus. *Science*, *322*, 1555–1559.
- Trussell, L. O., & Jackson, M. B. (1985). Adenosine-activated potassium conductance in cultured striatal neurons. *Proc Natl Acad Sci U S A*, *82*, 4857–4861.
- Vogt, A., Hormuzdi, S. G., & Monyer, H. (2005). Pannexin1 and pannexin2 expression in the developing and mature rat brain. *Brain Res Mol Brain Res*, *141*, 113–120.
- Wall, M. J., & Dale, N. (2013). Neuronal transporter and astrocytic ATP exocytosis underlie activity-dependent adenosine release in the hippocampus. *J Physiol*, *591*, 3853–3871.
- Wieraszko, A., Goldsmith, G., & Seyfried, T. N. (1989). Stimulation-dependent release of adenosine triphosphate from hippocampal slices. *Brain Res*, *485*, 244–250.
- Wieraszko, A., & Seyfried, T. N. (1989). Increased amount of extracellular ATP in stimulated hippocampal slices of seizure prone mice. *Neurosci Lett*, *106*, 287–293.
- Zappala, A., Cicero, D., Serapide, M. F., Paz, C., Catania, M. V., Falchi, M., Parenti, R., Panto, M. R., La Delia, F., & Cicirata, F. (2006). Expression of pannexin1 in the CNS of adult mouse: Cellular localization and effect of 4-aminopyridine-induced seizures. *Neuroscience*, *141*, 167–178.